13th World Conference on Earthquake Engineering
Vancouver, B.C., Canada
August 1-6, 2004
Paper No. 609

DEVELOPMENT OF REAL-TIME RESIDUAL SEISMIC CAPACITY EVALUATION SYSTEM -INTEGRAL METHOD AND SHAKING TABLE TEST WITH PLAIN STEEL FRAME-

Koichi KUSUNOKI [1] and Masaomi TESHIGAWARA[2]

SUMMARY

In order to reduce furthermore damage of structures and the number of refugee due to an aftershock, a quick inspection on the damaged buildings must be carried out. However, the buildings have to be investigated one by one by engineers or researchers under the present situation. The judgement can vary according to the engineers' experiences and it takes long time to investigate all damaged buildings. This research aims to develop a new automatic and quick inspection system that has only a few cheap accelerometers. This system makes it possible to indicate the safety level of a building against an aftershock to inhabitants immediately. The judgement will be made based on the spectrum method. In this paper, shaking table test results with steel frame structures are presented to confirm the validity of the system.

INTRODUCTION

Once a big earthquake occurs, many buildings are severely damaged, and consequently it gives rise to many homeless. The damage level could increase due to an aftershock in some buildings. Thus enormous harm to the inhabitants in such buildings could occur. On the contrary, some people could get caught up in fear and would escape from even the buildings that have enough residual seismic capacity from the engineering point of view. Hence, the number of homeless can increase drastically. In order to reduce further damage due to an aftershock and to reduce the number of homeless, a quick inspection on the damaged buildings must be carried out soon after a main shock. However, under the present situation, the buildings have to be investigated one by one by engineers or researchers. For example, 5,068 engineers and 19 days were needed to investigate 46,000 buildings on a damaged area at the Kobe earthquake (JBDP [1]). Nineteen days were too long and yet the number of investigated buildings was not enough. Moreover, many buildings were judged as "Caution" level, which needs detailed investigation by engineers. "Caution" judgement is a gray zone and it could not take away anxieties from inhabitants. Furthermore, the current quick investigation system presents a dilemma since buildings should be investigated by visual observation of engineers. Thus, this judgement varies according to the engineers' experiences.

---

[1] Senior Researcher of Building Research Institute, Japan, kusunoki@kenken.go.jp
[2] Chief Researcher of Building Research Institute, Japan, teshi@kenken.go.jp

On the other hand, if it is possible to calculate the performance and demand curve (JBRP [2]) from a measured acceleration of the basement and of each floor of a structure with cheap accelerometers, and further estimate the residual seismic capacity of a structure by comparing these curves, the problems mentioned above can be solved. To draw the performance curve, the absolute response accelerations and relative response displacement on each floor are needed. A certain fixture is generally needed to measure the inter-story drift or the relative response displacement to the basement. This fixture can be obstructive for usage. On the contrary, it is easy to measure accelerations with accelerometers. If displacements can be derived from the accelerations with double integral, the performance curve of structures can be easily measured.

In this paper, a new real-time residual seismic capacity evaluation system was proposed. Furthermore, shaking table tests with steel plane frame was carried out to confirm the validity of the proposed evaluation system.

CONFIGURATION OF THE SYSTEM AND OUTLINE OF THE EVALUATION

This system has basically two accelerometers and one judgement machine as shown in Fig. 1. The evaluation method is based on the performance design concept as shown in Fig. 2. The residual seismic capacity will be judged by comparing the measured performance curve of a structure and the measured demand curve.

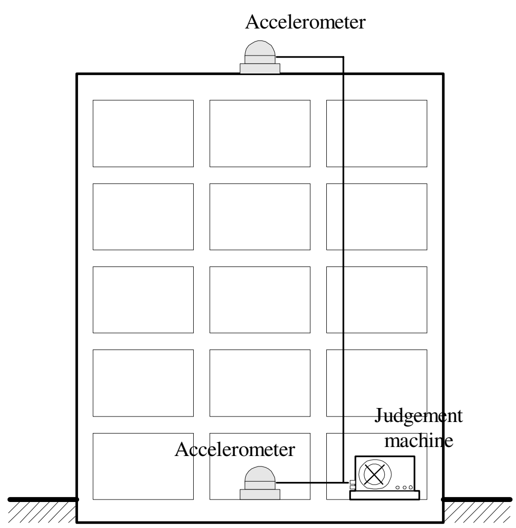

Fig. 1 Configuration of the system

The performance curve is the relationship between the representative deformation D and the representative restoring force S, which shows the predominant response of a structure. The method to evaluate theses representative values is outlined below.

The calculated relative displacement vector to the basement $\{_M x\}$ from measured accelerations can be derived as Eq. 1 with the modal participation factor $_M\beta$, mode vector $\{_M u\}$, and the assumption that the $\{_M x\}$ is the unique vibration mode.

$$\{_M x\} = {}_M\beta \cdot \{_M u\} \cdot \Delta \qquad \text{Eq. 1}$$

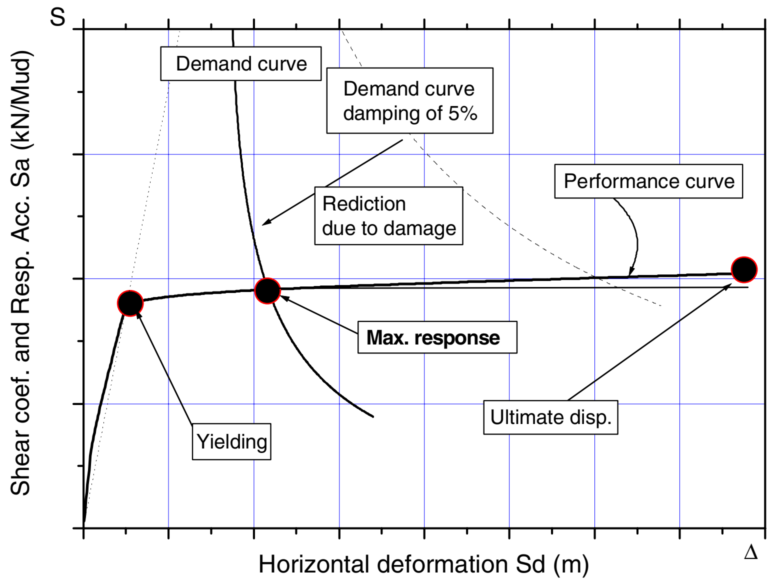

Fig. 2 Outline of the evaluation based on the Performance design concept

The story shear (inertia force) of the first story ${}_MQ_B$ can be calculated using Eq. 2 with the measured absolute acceleration $\{{}_M\ddot{x}+\ddot{x}_0\}$ and mass m_i of each floor.

$$ {}_MQ_B=\sum m_i\cdot({}_M\ddot{x}_i+\ddot{x}_0) \qquad \text{Eq. 2} $$

The equation of motion of a multi-degree-of-freedom system can be reduced to a single- degree-of-freedom system as given in Eq. 3.

$$ M\cdot\ddot{\Delta}+{}_M\tilde{C}\cdot\dot{\Delta}+{}_M\tilde{K}\cdot\Delta=-M\cdot\ddot{x}_0 \qquad \text{Eq. 3} $$

M	:	Total mass of a structure
${}_M\tilde{C}$	:	Equivalent damping
${}_M\tilde{K}$	:	Equivalent stiffness
$\ddot{x}_0$	:	Ground acceleration

The ${}_MQ_B$ can be calculated with Eq. 4. If the first mode is predominant enough, the calculated angular frequency, ${}_M\omega=\sqrt{\frac{{}_M\tilde{K}}{M}}$, can be the natural angular frequency of the first mode.

$$ S={}_MQ_B=M\cdot\ddot{\Delta} \qquad \text{Eq. 4} $$

Eq. 5 can be derived from Eq. 1 by deviding both sides by Δ. The inertia force acting on each floor ${}_MP_i$ can be derived as Eq. 6 by using Eq. 1 and Eq. 5.

$$ {}_M\beta\cdot{}_Mu_i=\frac{{}_Mx_i}{\Delta} \qquad \text{Eq. 5} $$

$$ {}_MP_i=m_i\cdot{}_M\beta\cdot{}_Mu_i\cdot\ddot{\Delta}=m_i\cdot\ddot{\Delta}\cdot\frac{{}_Mx_i}{\Delta} \qquad \text{Eq. 6} $$

The total mass M can also be derived from Eq. 4 and Eq. 6 since the total mass M is the sum of each floor mass, i.e.;

$$M = \frac{{}_M Q_B}{\ddot{\Delta}} = \frac{\sum m_i \cdot \ddot{\Delta} \cdot \frac{{}_M x_i}{\Delta}}{\ddot{\Delta}} = \frac{\sum m_i \cdot {}_M x_i}{\Delta} = \sum m_i$$

Therefore, the representative displacement Δ can be derived as Eq. 7.

$$\Delta = \frac{\sum m_i \cdot {}_M x_i}{\sum m_i} \qquad \text{Eq. 7}$$

The representative acceleration, $\ddot{\Delta}$ is applied to the representative restoring force, S ($S = {}_M Q_S / \sum m_i = \ddot{\Delta}$). If a system is elastic, the representative displacement, Δ and the representative acceleration, $\ddot{\Delta}$ can be calculated with Eq. 8, i.e.;

$$\ddot{\Delta}^2 + 2 \cdot {}_M h \cdot {}_M \omega \cdot \dot{\Delta} + {}_M \omega^2 \cdot \Delta = -\ddot{x}_0 \qquad \text{Eq. 8}$$

${}_M h$: Damping coefficient

${}_M \omega$: Angular frequency

As a result, the maximum representative displacement Δ_{max} and the absolute acceleration $(\ddot{\Delta} + \ddot{x}_0)_{max}$ correspond to the value from the response displacement and acceleration spectrum with a damping coefficient of ${}_M h$.

On the other hand, the demand curve is the relationship between the response acceleration (Sa) and displacement (Sd) spectrum. The intersection point of the demand and performance curve shows the maximum elastic response. However, the damage of a structure can dissipate some amount of an input energy, thus the damping effect can be increased. Therefore, the demand curve can be reduced according to the damage (**Fig. 2**). The intersection point of the reduced demand and performance curves shows the maximum inelastic response.

Additionally, the following three challenging assumptions were applied for the judgement of the residual seismic capacity. These assumptions need further studies.

Definition of aftershock
The mechanism of an aftershock is the same as the main shock, and the aftershock is always smaller than the main shock
With this assumption, the demand curve of the aftershock corresponds to the main shock.

Substitute damping ratio for aftershock and judgement
The damping coefficient for the demand curve of an aftershock is 5%
In fact, if further damage occurred in a structure during an aftershock, an additional damping can be achieved, then the demand curve will be reduced. However, it is difficult now to estimate accurately the damping effect due to the damage during an aftershock. Therefore, the damping effect due to inelastic behavior during an aftershock is neglected and 5% viscous damping is taken into account for the judgement on the safe side. The residual seismic capacity can be calculated with the comparison of the demand curve with 5% damping and the performance curve. If the ratio of the Sa(=Sa_p) at the ultimate

displacement on the performance curve to the Sa(=Sa_d) on the demand curve is greater than 1.0, the structure will be judged as SAFE, and if it is less than 1.0, it will be judged as UNSAFE.

The restoring force and the vibration mode will be constant after the maximum response is reached and less than the ultimate.

If the maximum response is less than the ultimate displacement, the performance curve to the ultimate displacement must be extrapolated. The restoring force and the vibration mode are assumed as constant after the maximum response reached to the ultimate displacement.

If a structure is elastic during a main shock, the performance curve calculated with the assumption (3) can be much underestimated since the restoring force at the ultimate displacement can be less than the yielding strength. Therefore, it must be judged separately if a structure is elastic. The elastic-inelastic judgement method is shown in Fig. 3. Firstly, the approximated stiffness of the envelope curve of the performance curve is calculated. Secondly, the error between the envelope curve and the approximated line, $\Delta Sd_{(i)}$, is calculated. If the ratio of the maximum value of, $\Delta Sd_{(i)}$, to the maximum response, Sd_{max}, is less than a tolerance, it is judged as elastic. In this study, a 5% tolerance is applied.

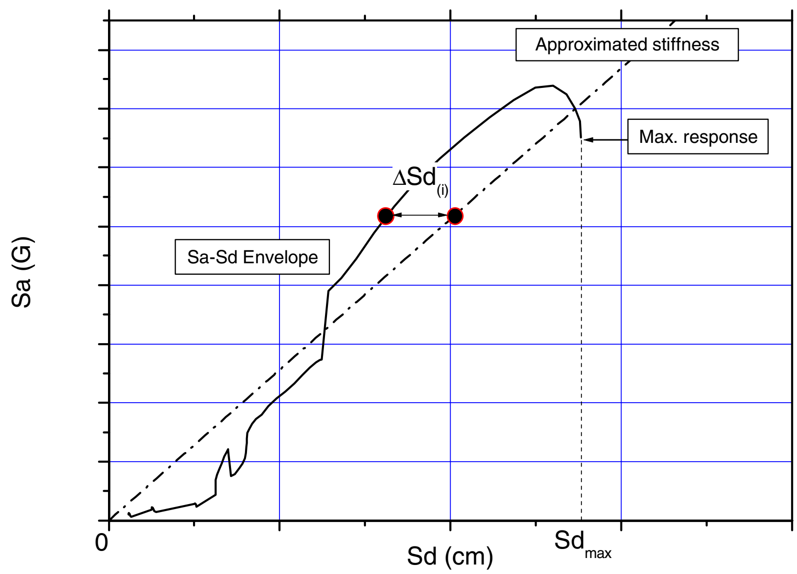

Fig. 3 Elastic-inelastic judgement

The judgement flowchart is shown in Fig. 4. The responses of a building and an input earthquake motion are measured by accelerometers, and the residual seismic capacity, i.e. how large the aftershock can be sustained by the building, is calculated from these measured accelerations. The safety level against an aftershock can be indicated just soon after a main shock. This System has a computer application, which can calculate the following items;

Integrate the measured accelerations twice to calculate the response displacements.

Calculate the base-shear coefficient and the representative displacement of the building with an assumed mode shape. (items 7 & 8 in Fig. 4)

Draw the performance curve of the structure. (item 9 in Fig. 4)

Draw the envelope curve of the performance curve. (item 10 in Fig. 4)

Calculate the response spectrum of the measured acceleration on the basement, and calculate the demand curve. (14 in Fig. 4)

Evaluate the residual seismic capacity of the building by means of the performance and demand curves.

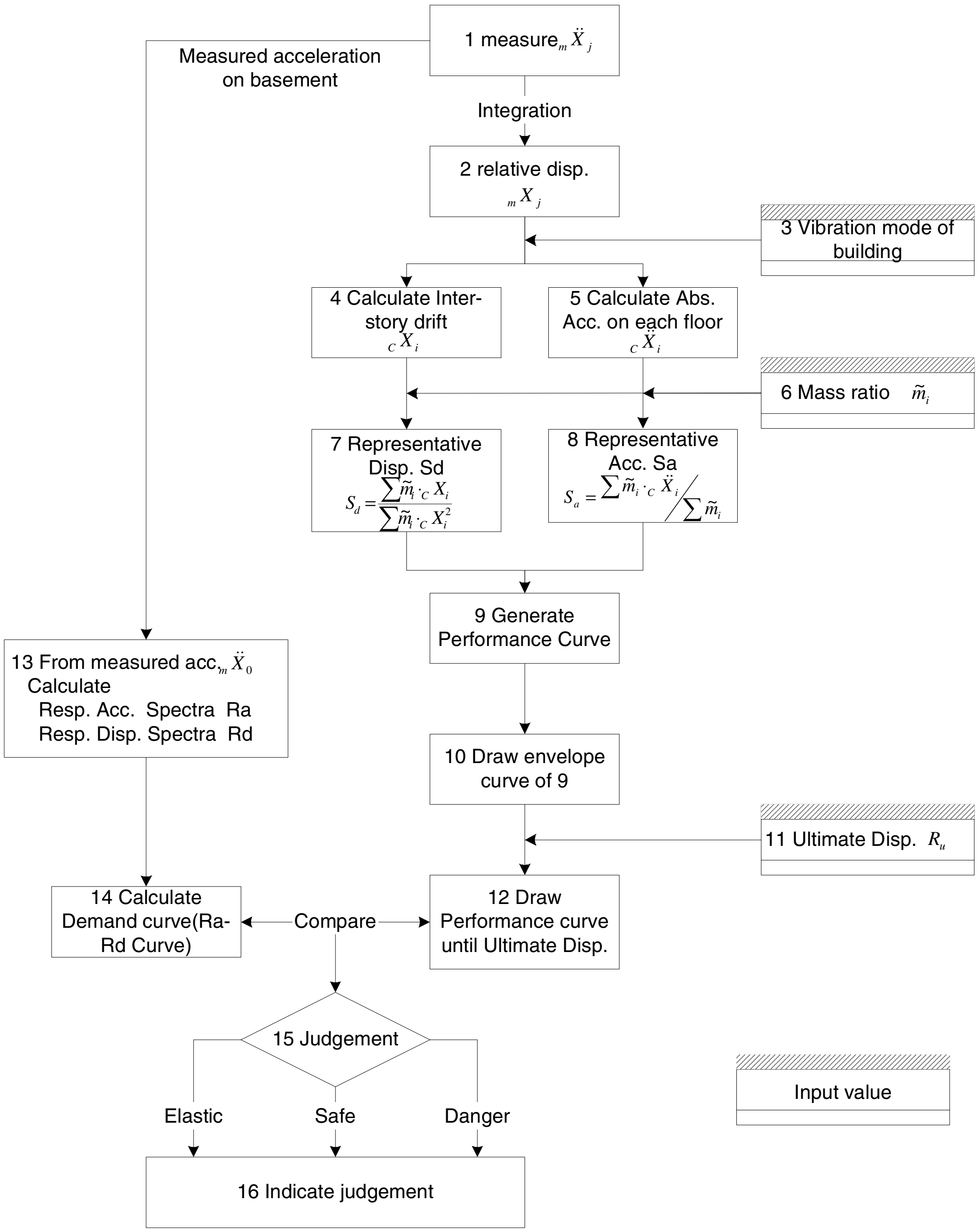

Fig. 4 Judgement flow chart

Items 3, 6, and 11 in Fig. 4 must be defined prior to making a judgement. The item 3 (vibration mode shape) is to calculate the response accelerations on the floors where there are no accelerometers. For example, a linear or a constant distribution shape between measured floors can be applied. The item 6 (mass ratio) can be calculated from floor area ratio between each floor. At the moment, item 11 (ultimate displacement) can be defined from the corresponding adopted building code.

INTEGRATION METHOD TO CALCULATE DISPLACEMENT FROM ACCELERATION

The response displacement is derived from measured acceleration with double integral technique in the proposed evaluation system. If displacement is calculated with the trapezoidal integral technique, it can diverge easily.

There are two ways to integrate acceleration record, integration in frequency-domain and in time-domain. The Iwan's method (Iwan [3]) was applied for the system, which integrates in time-domain. The outline of Iwan's method is described below.

The noise level observed during a principal shock is assumed to be constant. The noise level before and after a principal shock are also assumed to be constant but different values. The noise level before a principal shock can be calculated as the average of measured acceleration record until the principal shock starts. At first, the calculated noise level before the principal shock is subtracted from whole measured acceleration record. Then adjusted acceleration record is integrated to calculate time history of velocity (**Fig. 5**). The velocity baseline shift after a principal shock is calculated with linearization technique so that the velocity can be zero at enough after the principal shock. The velocity baseline shift during the principal shock can be calculated so that the velocity baseline shift due to the noise level can continue from the principal shock domain to after the principal shock domain.

The measured acceleration from the shaking table test of the 3-story steel structure, and the integrated displacement without using the Iwan's method are shown in **Fig. 6**. The calculated velocity baseline shift by using Iwan's method mentioned above is shown in **Fig. 7**, and the acceleration baseline shift is shown in **Fig. 8**. It is obvious from **Fig. 7**that the calculated velocity baseline shift is not appropriate. The time-history of the adjusted velocity is elbowed during the principal shock, and the calculated displacement from the elbowed velocity can include much error. It can be the reason why several strong pulses are observed during the principal shock in **Fig. 6**, and the baseline shift could occur at each pulse because of the non-linearity of the accelerometers. Because of that, the baseline shift during the principal shock could not be represented by the constant acceleration.

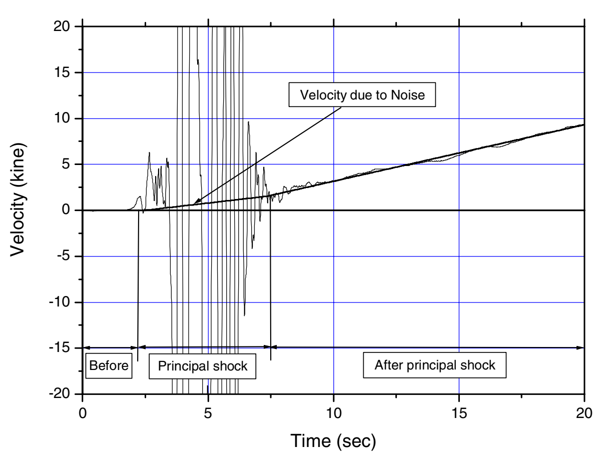

Fig. 5 Iwan's integration method (velocity)

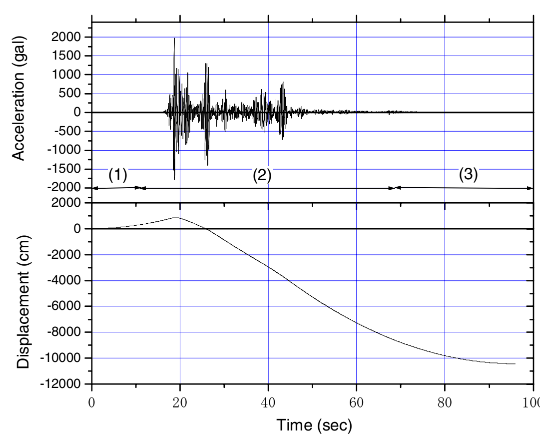

Fig. 6 Measured acceleration and the integrated displacement

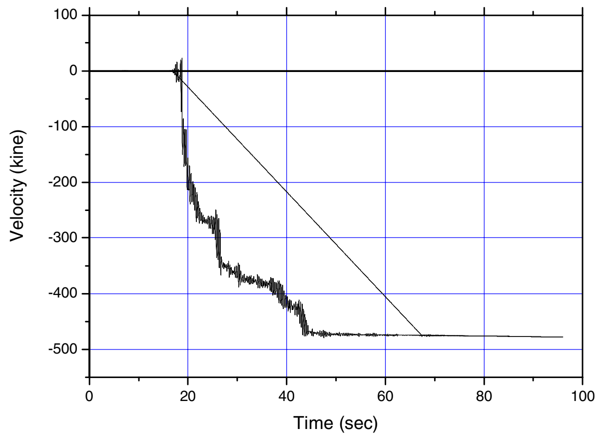

Fig. 7 Velocity without initial acceleration baseline shift and velocity baseline shift

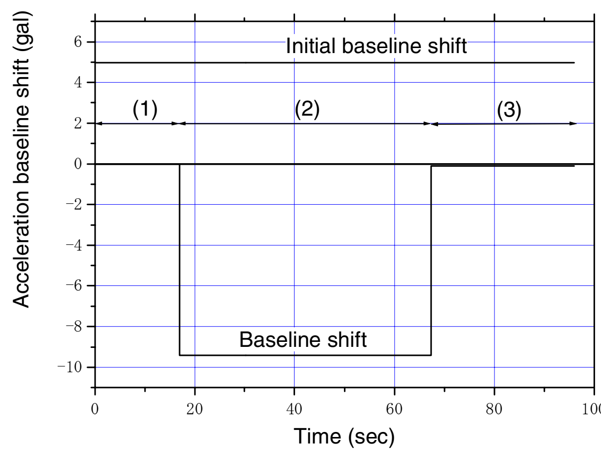

Fig. 8 Calculated baseline shift

Fig. 9 shows the Fourier amplitude of the integrated displacement from the time history of the elbowed velocity. It can be observed that it contains much low-frequency (long period) components because of the elbowed shaped velocity. In order to remove the error components in frequency-domain, the proper lower and upper bound frequencies ω_L and ω_H must be found automatically. The proposed method to find out ω_L and ω_H is described below.

Firstly, the power spectrum of the adjusted velocity with the Iwan's method is smoothed with the Parzen's Spectral Window (Osaki [4]) (**Fig. 10**). Secondly, the frequencies ${}_{min}\omega_i$ when the Fourier amplitude is a local minimum are found. Sometimes more than one ${}_{min}\omega_i$ can be found. Three ${}_{min}\omega_i$ were shown in **Fig. 10**. Thirdly, the frequencies ${}_{max}\omega_i$ when the Fourier amplitude is a local maximum between ${}_{min}\omega_i$ and ${}_{min}\omega_{i+1}$, and the difference of the Fourier amplitudes at ${}_{min}\omega_i$ and ${}_{max}\omega_i$, h_i, can be calculated. The ${}_{min}\omega_i$ of which h_i is the maximum is applied for the ω_L. Since the h_2 was the maximum in **Fig. 10**, the ω_L was calculated as 1.8066 Hz. If the Fourier amplitude at the first natural frequency is enough greater than the Fourier amplitude at the ω_L (F_2 in **Fig. 10**), an appropriate ω_L can be found. If it is not enough greater, a higher degree function must be applied to calculate baseline shift during a principal shock. If a measured acceleration contains no error, the ω_L is calculated as 0 Hz since the power spectrum shows monotone increasing function from 0 Hz to the first natural frequency.

The upper bound frequency ω_H was defined as 25 Hz since the frequency characteristic of the accelerometer (frequency bandwidth able to be measured) was from a DC up to 30Hz.

Finally, the Butterworth filter, which is a kind of band-pass filter, with its parameter of 4 (Boore [5]) was applied for the Fourier spectrum of the calculated velocity with the Iwan's method from ω_L to ω_H. The Fourier spectra with and without the Butterworth filter are shown in **Fig. 11**. The displacement can be calculated from the velocity, which is inversely Fourier transferred from **Fig. 11**. The calculated displacement of the measured acceleration shown in **Fig. 6** and measured displacement during the shaking table test are shown in **Fig. 12**. It can be observed that the calculated displacement agreed well with the measured displacement.

It can be thought to use the band-pass filter for the displacement without the Iwan's method shown in **Fig. 6**. However, if the Iwan's method was not applied, the effect of noise can be big enough so that the component of real vibration can hide behind the noise components in the Fourier. In other words, the Iwan's method must be applied to reduce the noise components so that the ω_L can be clearly observed.

The proposed method to find out the ω_L is utilizing the characteristic of the structural vibration of which natural frequency can be clearly found in the Fourier spectrum. Therefore, the proposed method has to be used carefully in case of integrating a measured ground acceleration since it has many and random predominant frequencies.

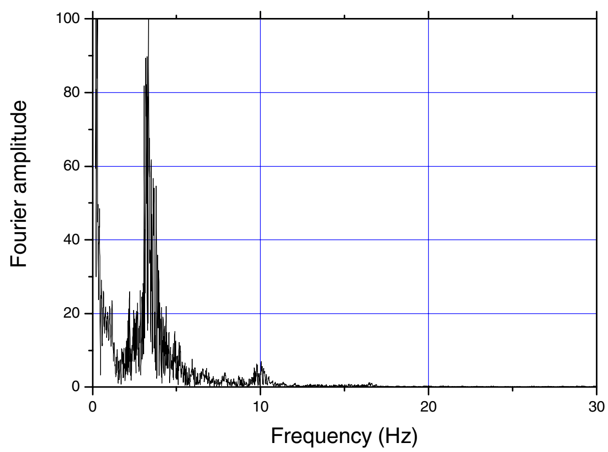

Fig. 9 Fourier amplitude of the integrated displacement (Iwan's method)

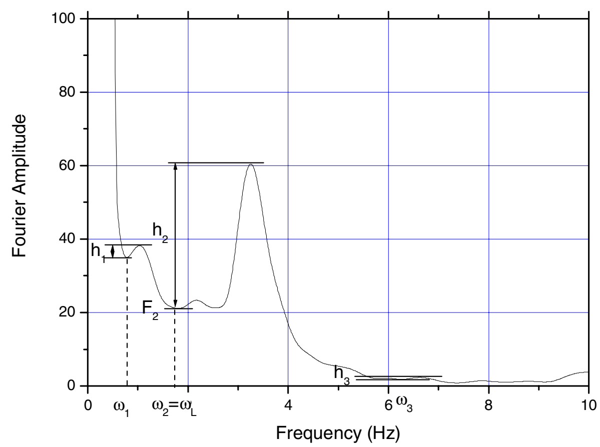

Fig. 10 How to find the ω_L

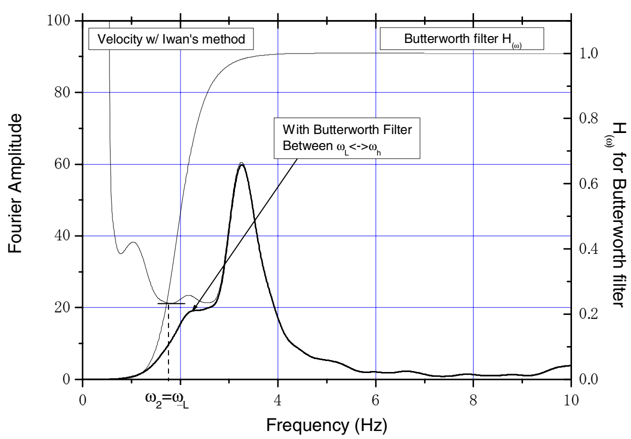

Fig. 11 Comparison of Fourier spectra

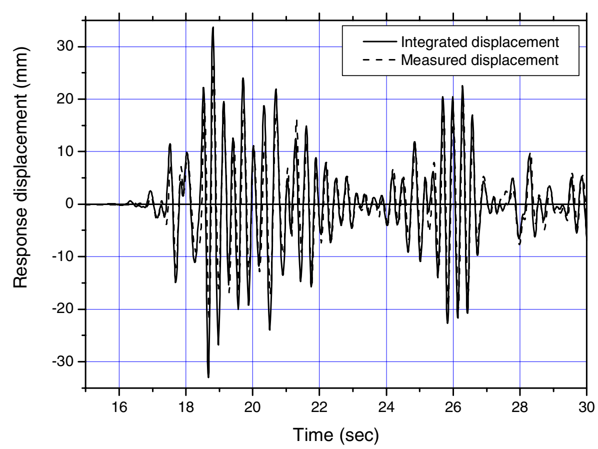

Fig. 12 Integrated displacement with band-pass filter and measured displacement

APPLICABILITY WITH THE SHAKING TABLE TEST RESULTS

Test specimens

The specimens were one span plane steel frame structure of which masses are concentrated to the nodal points. Steel plats, of which width was 100mm and thickness was 6mm, were used for columns and beams. The number of story was 1, 2, and 3. The 3-story specimen is shown in **Fig. 13**. The span length was 1,000mm and the story height was 595mm for the first story and 600mm for the second and third story. The weight at the nodal point was 190 N.

Two different failure modes of specimen, story failure in the first story and total yielding failure (both ends of beams and bottom of the first story columns yield, referred to as total failure, subsequently) were expected. In order to achieve the expected failure, the low-yield strength steel (nominal strength is 100 N/mm^2, referred to as YL100, subsequently) was used for the yield members, and the ordinal strength steel (nominal strength is 400 N/mm^2, referred to as SN400, subsequently) was applied for the not-yield members. The material test results are listed in **Table 1**. The average yield strength of YL100 was 72.4 N/mm^2, and 315.8 N/mm^2 for SN400. The lateral strength of each specimen was calculated with these average strengths listed in **Table 1** based on the principle of virtual work. The base shear coefficient of each specimen is listed in **Table 2**. Single story had high base shear coefficient of 0.67. On the other hand, the value for other specimens were relatively low as not exceeding 0.30.

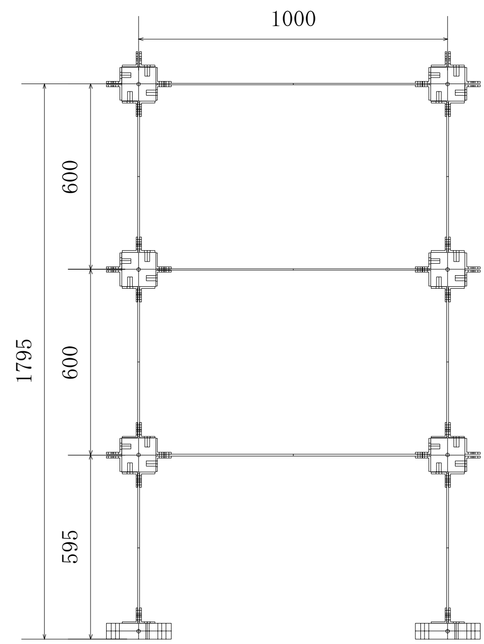

Fig. 13 Test specimen (3-story)

Table 1 Material properties

	Case	Young's module (N/mm^2)	Yield stress (N/mm^2)	Yield Strain (μ)	Fracture stress (N/mm^2)
LY100	1	192094.3	74.9	390.0	274.5
	2	174524.6	72.4	414.9	272.9
	3	179168.2	69.7	389.2	192.4
	Average	181929.0	72.4	398.0	246.6
SN400	1	197300.2	310.2	1572.2	443.6
	2	198195.8	312.2	1575.2	440.6
	3	197165.3	325.1	1648.9	441.5
	Average	197553.8	315.8	1598.8	441.9

Table 2 Base shear coefficient of each specimen

	Single story	2-story	3-story
Story failure	0.67	0.22	0.11
Total failure	0.67	0.30	0.19

The NS component of the El Centro earthquake record was used for the input motion. The 5% PGA level of the record was inputted first. Then the input level was increased by 5% up to the maximum capacity of the shaking table, 180%. The input motion is shown in **Fig. 14**, and the Sa-Sd curve (demand curve) is shown in **Fig. 15**. The elastic response line with natural period of 0.5 is also shown in the figure.

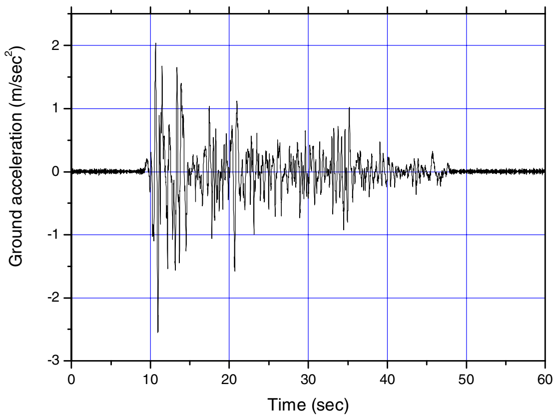

Fig. 14 Input motion (100% amplification)

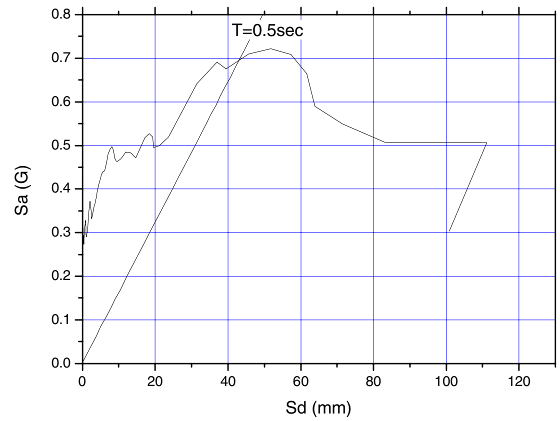

Fig. 15 Sa-Sd curve for the input motion (100% amplification)

Measurement

The measuring system is shown in **Fig. 16**. Each story had an accelerometer on the center of the beam to measure the response acceleration and to be used for double integral to calculate displacement. Another accelerometer was also placed on the surface of the shaking table to measure the actually inputted motion. The response displacements of each floor and the shaking table were also measured by transducers to confirm the accuracy of the integrated displacement and of the performance curve with the integrated displacement.

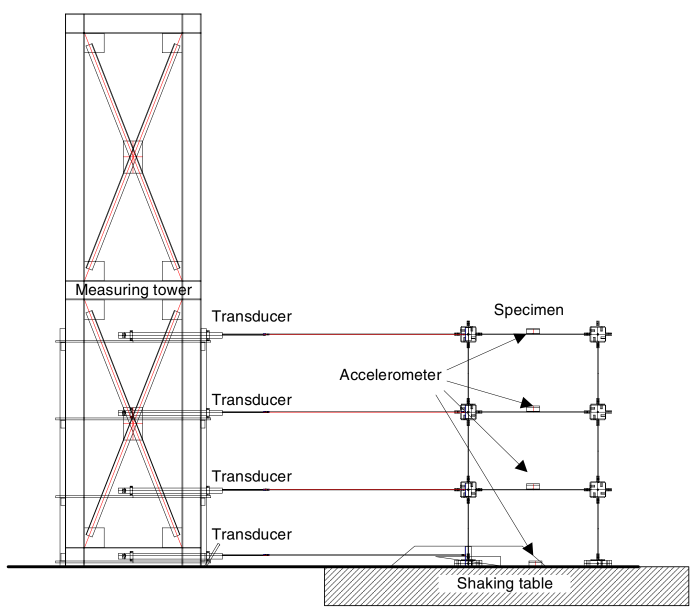

Fig. 16 Measuring system

The measuring frequency of 100Hz was applied. The measurement was automatically started with the system start trigger of 50 mm/sec^2 (5 gal). If an accelerometer senses acceleration of more than 5 gal, the measurement system was started. Since the accelerometer system has a memory, the record from 5 seconds prior to the triggered time was also stored. Then when the measured acceleration did not exceed 50 gal for 10 seconds, the measurement was automatically stopped and the residual seismic capacity evaluation program was executed.

For the evaluation, the ultimate deformation angle was assumed as 0.1%. For the double integral, the principal input motion ((2) portion in **Fig. 6**) was assumed to start when the measured acceleration exceeds 5 gal, and to end when the measured acceleration did not exceeds 50 gal subsequently.

Test results and discussions

The performance curve of the 2-story total failure specimen calculated with integrated displacement from measured acceleration and the curve with measured displacement are shown in **Fig. 17**. The input level was 50% of the original record. The demand curve calculated from the measured acceleration on the surface of the shaking table is also superimposed in the figure. The specimen was judged ELASTIC. The strength of the 2-story total failure specimen was calculated as 0.3 (**Table 2**). The measured maximum base shear coefficient exceeded 0.3 a little bit, however from **Fig. 17**, it can be seen the specimen is still elastic or just yielded. The performance curve with the displacement from the measured acceleration agreed very well with the curve with the measured displacement.

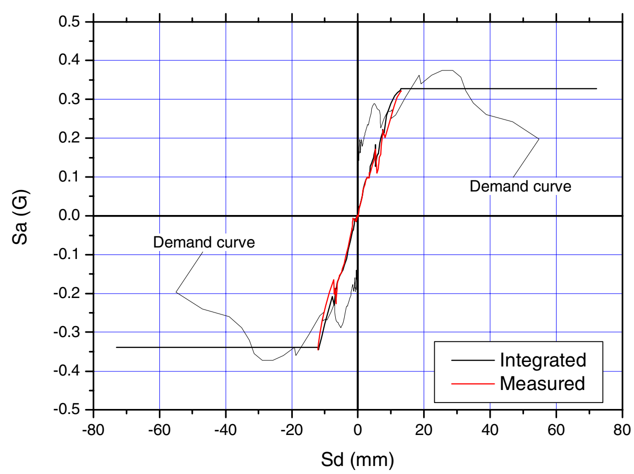

Fig. 17 Envelope of the Sa-Sd curve (2-story, total failure, 50% input amplification)

Fig. 18 shows the both performance curves of the 3-story story failure specimen. The input level was the 110% of the original record. The integrated maximum displacement was 57mm in the positive direction. The performance curve with the integrated displacement was extended horizontally from the recorded maximum displacement point to the assumed ultimate displacement. The specimen was judged UNSAFE, since it was evaluated inelastic and the expected ultimate point was less than the demand curve with 5% damping. The ratio of the ultimate point to the demand curve (residual seismic capacity ratio) was calculated as 0.836. This value shows that the specimen will survive after the aftershock of which level is 83.6% of the main shock. Even the specimen was inelastic and response displacement was relatively big, the performance curve with displacement from measured acceleration agreed acceptably with the curve with measured displacement.

Fig. 19 shows the response and integrated response displacement on the top of the specimen. The integrated displacement from the measured acceleration agreed very well with the measured displacement.

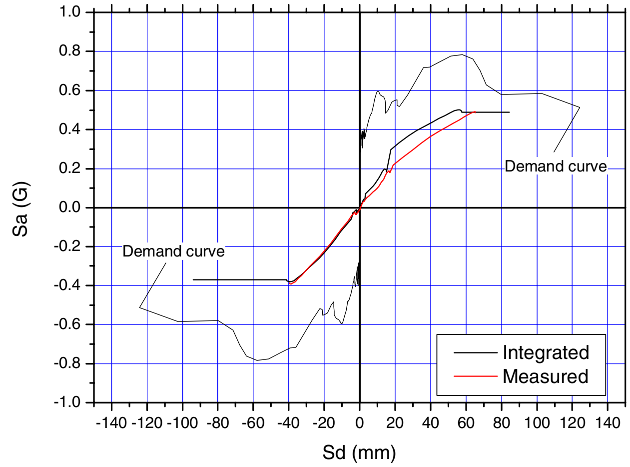

Fig. 18 Envelope of the Sa-Sd curve (3-story, story failure, 110% input amplification)

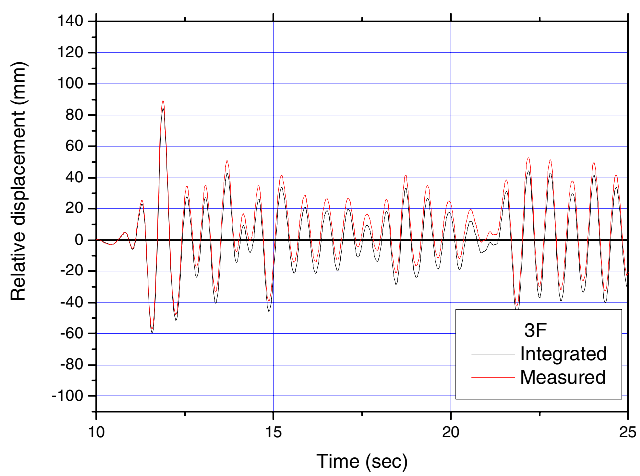

Fig. 19 Relative displacement history on the 3rd floor (3-story, story failure, 110% input amplification)

In order to make a severe damage to the 2-story story failure specimen, the sectional area of the column was reduced. **Fig. 20** shows Sa-Sd curves with integrated and measured displacements. The Sa-Sd curve with integrated displacement is less than the curve with measured displacement in the negative direction. **Fig. 21** shows the integrated and measured relative displacements to the shaking table on the top of the specimen. It can be seen that large residual displacement occurred in the negative direction because of the yielding. However, the residual displacement could not be seen in the integrated displacement, since the band-pass filter is applied during the integration and the long period portion is cut off.

Although the Sa-Sd curves shown in **Fig. 20** are different, the envelope curve of the Sa-Sd curve agreed well as shown in **Fig. 22**. Since the evaluation is carried out with the performance curve (envelope curve of the Sa-Sd curve), if the yielding displacement and strength are predicted well from the measurement, the accuracy of the evaluation can be acceptable. Thus, the difference of the residual displacement can be not effective to the evaluation result.

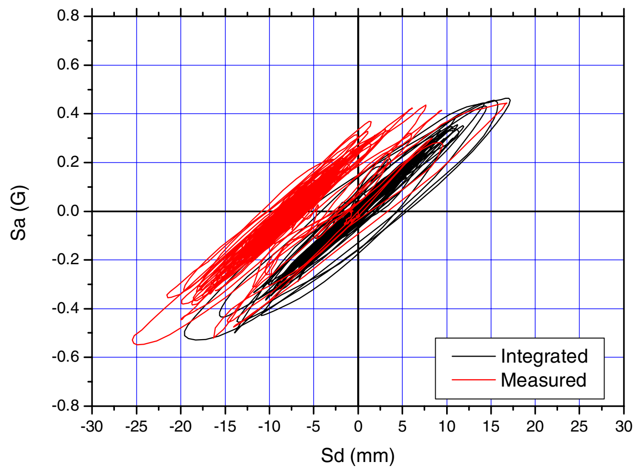

Fig. 20 Sa-Sd curve (2-story, story failure, 180% input amplification, column section was reduced)

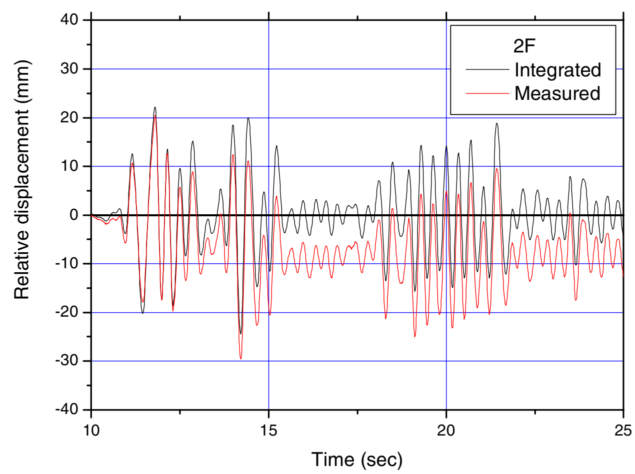

Fig. 21 Relative displacement history on the 2nd floor (2-story, story failure, 180% input amplification, column section was reduced)

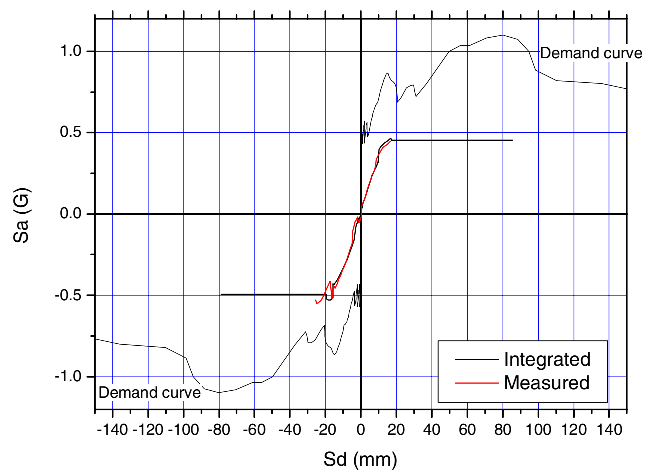

Fig. 22 Envelope of the Sa-Sd curve (2-story, story failure, 180% input amplification, column section was reduced)

CONCLUDING REMARKS

In order to develop the real-time residual seismic capacity evaluation system for improving the safety against an aftershock, the outline of the evaluation system, the evaluation results with existing shaking table results. Results obtained from the investigation can be summarized as follows;

1. The new residual seismic capacity evaluation method was proposed.
2. The Iwan's integration method cannot remove errors enough for some acceleration record. However, the band-pass filter can remove the errors, which cannot be removed with the Iwan's method.
3. The new integration method with the algorithm to find out the lowermost frequency for the band-pass filter is proposed.
4. Since the proposed integration method utilizing the characteristic of the structural vibration in which predominant frequencies can be found obviously, more attention must be paid in case of using the proposed method to integrate ground acceleration.
5. The integrated displacements from the measured acceleration at the shaking table test agreed very well with the measured displacements. However, the residual displacement on the shaking table did not agree well with the measured displacement.
6. The difference of the residual displacement cannot affect the residual seismic capacity evaluation result done by the proposed system.
7. The envelope of the performance curve calculated with the integrated displacement agreed very well with the measured envelope curve.
8. The validity of the proposed evaluation system was demonstrated with shaking table test results of 1 bay 1 to 3 story steel frame specimens.

REFERENCES

1. Building Center of Japan (BCJ), Report on the reconnaissance committee on the building damages due to the Hanshin-Awaji Great Earthquake Disaster, 1995 - Summerization -, 1996.3 (in Japanese)
2. Japan Building Research Promotion Association (BRPA), Guidelines for performance evaluation of reinforced concrete buildings, Gihodo, 2000.7 (in Japanese)
3. Iwan, W. D., et al. : Some Observations on Strong-motion Earthquake Measurement using a Digital Accelerograph, Bulletin of the Seismological Society of America, Vol. 75, pp. 1255-1246, 1985.10
4. M. Osaki, Revised manual for the spectral analysis for eathquake, Kashima-Syuppankai, 1994 (in Japanese)
5. David M. Boore, Christopher D. Stephens, and William B. Joyner, Comments on baseline correction of digital strong-motion data: Examples from the 1999 Hector Mine, California, earthquake, BSSA, Vol. 1.3, 2001.12
6. Koichi KUSUNOKI and Masaomi TESHIGAWARA, A new acceleration integration method to develop a real-time residual seismic capacity evaluation system, Journal of structural and construction engineering, Architectural Institute of Japan, No. 569, pp.119-126, 2003.7 (in Japanese)